RSC Advances

PAPER

View Article Online
View Journal | View Issue

Cite this: *RSC Adv.*, 2019, **9**, 6021

A novel diarylethene-based fluorescent "turn-on" sensor for the selective detection of Mg^{2+}†

Zhen Wang, Shiqiang Cui,* Shouyu Qiu and Shouzhi Pu*

Received 21st December 2018
Accepted 13th February 2019

DOI: 10.1039/c8ra10470k

rsc.li/rsc-advances

A new photochromic diarylethene derivative with a 4-methylphenol unit has been designed and synthesized. It displayed distinct photochromism and fluorescent "turn on" features to Mg^{2+} in acetonitrile solution. With the addition of Mg^{2+}, there was an obvious increase of fluorescent emission intensity at 552 nm, accompanied by a clear change of fluorescent color from dark purple to green. Meantime, the 1 : 1 stoichiometry between the derivative and Mg^{2+} was verified by Job's plot and HRMS. Furthermore, the sensor was successfully applied in the detection of Mg^{2+} in practical samples. Moreover, based on the multiple-responsive fluorescence switching behaviors, it also could be used to construct a molecular logic circuit with UV/vis lights and Mg^{2+}/EDTA as input signals and the emission at 552 nm as the output signal.

Introduction

Magnesium, as the fourth most plentiful cation in the human body, has been considered as an important biological ion for all living things in the past century.[1–8] Meanwhile, it plays significant physiological roles in numerous cellular processes, such as enzymatic catalytic reactions, membrane protein activities including ion channels, and the regulation of Ca^{2+} signal.[9–13] Moreover, magnesium plays a positive role in bone reconstruction and skeletal development.[14–16] Abnormal levels of magnesium in serum or cells have been associated with a variety of diseases, including cardiovascular disease, diabetes, neurodegeneration and cancer.[17–20] For instance, chronic magnesium deficiency may cause a lot of chronic diseases, such as diabetes, osteoporosis, hypertension and coronary heart disease.[21,22] On the contrary, high levels of Mg^{2+} can lead to many age-related and neuronal diseases ranging from high blood pressure to Alzheimer's disease.[23–25] In this regard, developing efficient and sensitive analytical methods for Mg^{2+} has attracted more and more interest in the biological sciences and chemistry.

In tradition, there are some analytical methods such as atomic absorption spectrum, ion-selective electrodes (ISES), and NMR for the detection of Mg^{2+}.[26–29] However, all of these methods need complex apparatus and high cost. So, the convenient and inexpensive method for the detection of Mg^{2+} in different environments is desired. Compared to these methods, fluorescence analysis is a very reliable and effective method to detect metal ions because of their high sensitivity, good selectivity, high reaction speed, and simple operation.[30–32] Up to now, various fluorescence sensors for Mg^{2+} have been developed. These sensors have different receptor groups based on moieties including diaza-18-crown-6,[33] benzo-15-crown-5,[34] calix[4]arene,[35] benzo-chromene,[36] imidazo-1,10-phenanthroline,[37] and other functional units.[38–42] However, most of the reported Mg^{2+} sensors have poor selectivity to Mg^{2+} and Ca^{2+}, due to their similar chemical properties, especially when the concentration of Ca^{2+} is much higher than that of Mg^{2+}. Hence, it is vital to design highly selective, sensitive, and simple sensors that can recognize Mg^{2+} without the interference of Ca^{2+}.[43,44]

Among the reported fluorescence sensors,[45–54] diarylethene derivatives are the most promising candidates owing to their excellent thermal stability, remarkable fatigue resistance, and rapid response time.[55–57] Furthermore, the recognized ions could induce a stable transformation between diarylethene molecule and complex, and these properties make it possible for the application in logic gates.[58] Although much work in diarylethenes based on ion recognition has been finished,[59–65] the sensors for the selective detection of Mg^{2+} based on diarylethenes are rarely reported.[66]

Herein, a new diarylethene-based fluorescent sensor (**1o**) for Mg^{2+} was developed. By investigating the fluorescent spectrum and color changes of this sensor under the stimulation of chemical substance and lights in acetonitrile solution, it could be found that the fluorescence of **1o** could be effectively regulated by Mg^{2+} and lights. Moreover, a systematic discussion of its photochromic and fluorescent properties was also recorded in the full text in detail.

Experimental

General methods

All the reagents used in the synthesis process were from a variety of commercial sources without further purification. All

Jiangxi Key Laboratory of Organic Chemistry, Jiangxi Science and Technology Normal University, Nanchang 330013, PR China. E-mail: cuisq2006@163.com; pushouzhi@tsinghua.org.cn; Fax: +86-791-83831996; Tel: +86-791-83831996

† Electronic supplementary information (ESI) available. See DOI: 10.1039/c8ra10470k

cations were added in the form of their corresponding metal nitrates except for Sn^{2+} and Hg^{2+} (their counter anion ions were chloride ions). Metal ion solutions (0.1 mol L^{-1}) were prepared by dissolving their respective metal salts in deionized water while performing the necessary dilutions according to each experimental device. Nuclear magnetic resonance hydrogen and carbon spectra were obtained with a Bruker AV400 spectrometer by using acetonitrile-d_3 as the solvents and tetramethylsilane (TMS) as an internal standard. High resolution mass spectrometry was collected on a Bruker Amazon SL ion trap mass spectrometer (ESI). The melting point was determined by a WRS-1B melting point instrument. UV-vis absorption spectra were recorded with an Agilent 8453 UV/vis spectrometer. Fluorescence spectra were measured by using a Hitachi F-4600 fluorescence spectrophotometer with the slit width of 5.0 nm for both excitation and emission. Photoirradiation experiments were performed with an SHG-200 UV lamp and BMH-250 visible lamp. Absolute fluorescence quantum yields were measured using an Absolute PL Quantum Yield Spectrometer QYC11347-11. Infrared spectra were collected on a Bruker Vertex-70 spectrometer. The pH was measured with Ferromagnetic PHS-3C pH meter. All of experiments were conducted at room temperature without special instructions.

Synthesis of compound 1o

Compound **2** was synthesized according to the method reported in the previous work.[67] Then compound **2** (0.094 g, 0.2 mmol) was dissolved in 5.0 mL absolute methanol, followed by the addition of 2-amino-4-methylphenol (0.025 g, 0.2 mmol). After the mixture was stirred at room temperature for 6.0 hours, the reaction system was placed in a freezer for overnight freezing (Scheme 1). It can be seen that a yellow solid precipitated and was washed three times with anhydrous methanol (5.0 mL × 3) and dried to get the target compound **1o** (0.096 g, yield: 83%). Mp: 435–437 K. ^{1}H NMR (400 MHz, acetonitrile-d_3, TMS), δ (ppm): 2.02 (s, 3H), 2.12 (s, 3H), 2.24 (s, 3H), 2.29 (s, 3H), 6.84 (d, J = 8.4 Hz, 1H), 7.04 (d, J = 8.6 Hz, 1H), 7.32 (s, 2H), 7.58 (s, 1H), 8.08 (d, J = 8.6 Hz, 1H), 8.40 (d, J = 8.4 Hz, 1H), 8.79 (s, 1H), 8.94 (s, 1H) (Fig. S1†). ^{13}C NMR (100 MHz, acetonitrile-d_3, TMS), δ (ppm): 10.7, 12.2, 14.6, 20.3, 105.0, 115.2, 115.9, 122.4, 125.5, 125.8, 130.2, 130.9, 133.9, 135.6, 139.3, 144.6, 147.1, 147.6, 151.2, 154.6, 157.9, 159.1, 171.1 (Fig. S2†). HRMS: m/z = 578.1313 $[M + H^+]^+$. Calcd 578.1337 (Fig. S3†).

Results and discussion

Photochromism of 1o

Fig. 1 shows the photochromic properties of **1o** by UV/vis light studied in acetonitrile (2.0×10^{-5} mol L^{-1}) at room temperature. Two absorption bands of compound **1o** at 338 nm ($\varepsilon = 2.94 \times 10^4$ mol^{-1} L cm^{-1}) and 381 nm ($\varepsilon = 2.67 \times 10^4$ mol^{-1} L cm^{-1}) were observed, respectively. When irradiated with 297 nm light, the ring-closed isomer **1c** was regenerated and a new absorption band centered at 536 nm ($\varepsilon = 1.93 \times 10^3$ mol^{-1} L cm^{-1}) appeared, owing to a larger π-electron delocalization formed in the molecule.[68] When the photostationary state (PSS) was reached, an isosbestic point was observed at 407 nm, indicating a reversible two-component photochromic reaction.[69] At the same time, there was a visible change of the color from colorless to pink. On the contrary, when irradiated with visible light (λ > 500 nm), the absorption spectrum and the color of the solution could be quickly recovered to that of **1o**. The cyclization and cycloreversion quantum yields of **1o** were determined to be 0.023 and 0.004, respectively, with 1,2-bis(2-methyl-5-phenyl-3-thienyl)perfluorocyclopentene as a reference[70] On the other hand, the fatigue resistance of **1o** was measured in acetonitrile by alternative irradiation of UV/vis lights at room temperature. The results showed that 10 times coloration–decoloration cycles between **1o** and **1c** could cause 20% degradation (Fig. S4†).

Selectivity of 1o to metal ions

The experiments of fluorescence selectivity of **1o** toward various metal ions (5.0 equiv. of **1o**) such as Al^{3+}, Cu^{2+}, Sn^{2+}, Ca^{2+}, K^+, Ag^+, Ni^{2+}, Ba^{2+}, Zn^{2+}, Mn^{2+}, Cd^{2+}, Sr^{2+}, Hg^{2+}, Co^{2+}, Cr^{3+}, Fe^{3+}, Pb^{2+}, and Mg^{2+} in acetonitrile were performed. As shown in Fig. 2, upon excitation at 350 nm, the fluorescence of **1o** was notably changed only when Mg^{2+} was added. The addition of other metal ions resulted in no obvious effects on the fluorescence emission of **1o**, except for the addition of Cd^{2+}. These results showed the ability of **1o** for distinguishing Mg^{2+} from other metals ions. Therefore, the diarylethene **1o** could be used as a selective fluorescent sensor for Mg^{2+} in acetonitrile. In addition, the experiments of fluorescence response of **1o** to Mg^{2+} in aqueous solution were also performed. As shown in Fig. S5,† there are no obvious changes in fluorescence with the addition of Mg^{2+}, due to the poor water solubility of **1o**.

Fluorescence studies of 1o toward Mg^{2+}

The fluorescence titration experiment of **1o** toward Mg^{2+} in acetonitrile was also investigated. As shown in Fig. 3A, **1o**

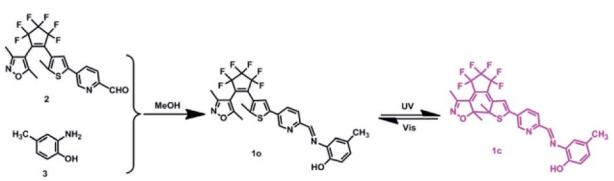

Scheme 1 The synthetic route and photochromism of **1o**.

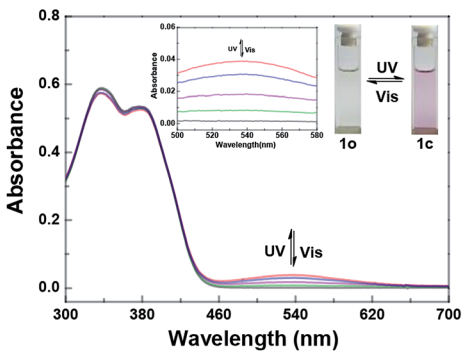

Fig. 1 Changes in the absorption spectra of **1o** upon irradiation with UV/vis lights in acetonitrile (2.0×10^{-5} mol L^{-1}).

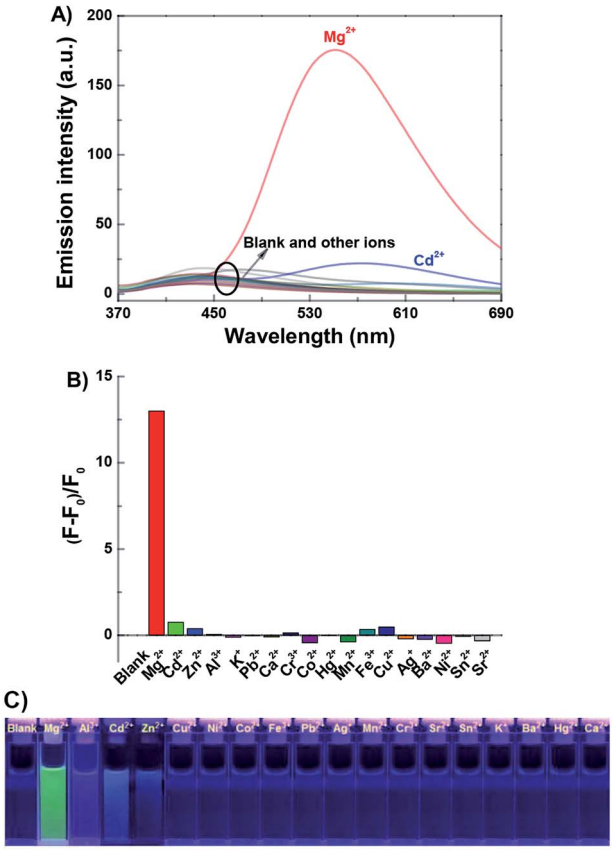

Fig. 2 Upon addition various metal ions to **1o** (2.0×10^{-5} mol L^{-1} in acetonitrile): (A) fluorescence emission spectral changes; (B) emission intensity changes; (C) fluorescent photos (λ_{ex} = 350 nm).

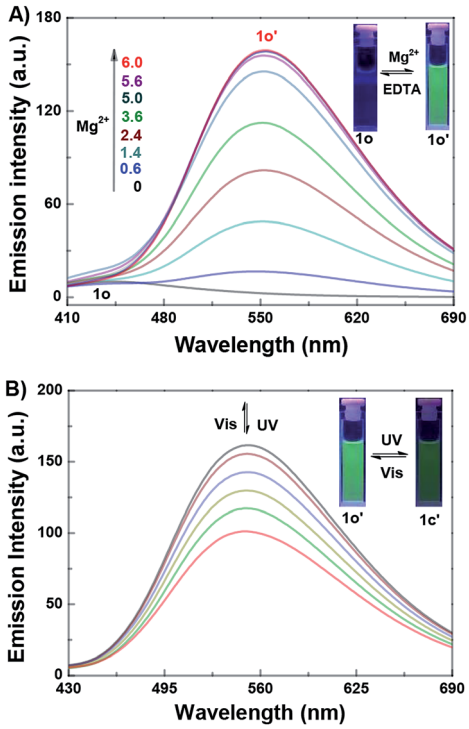

Fig. 3 (A) Fluorescence spectral changes of **1o** (2.0×10^{-5} mol L^{-1} in acetonitrile) induced by Mg^{2+} (0–6.0×10^{-5} mol L^{-1}); (B) fluorescence spectral changes of **1o′** (2.0×10^{-5} mol L^{-1} in acetonitrile), upon irradiation with UV/vis lights (λ_{ex} = 350 nm).

exhibited a very weak emission at 442 nm with 350 nm excitation. With the gradual addition of Mg^{2+}, the emission increased inch by inch, accompanied by a clear red shift from 442 nm to 552 nm. When the amount of Mg^{2+} reached to 3.0 equivalents of **1o**, the fluorescence intensity achieved its maximum (Fig. S6†), and the absolute quantum yield of fluorescence was determined to be 0.013. At the same time, the fluorescent color changed from dark purple to green, which was coincident with the changes in the fluorescence spectra. Reversely, with the addition of EDTA (10.0 equivalents of **1o**), the fluorescence spectrum recovered gradually to that of **1o**, indicating that the complexation reaction between **1o** and Mg^{2+} was reversible. The weak fluorescence of the original **1o** was attributed to the C=N bond isomerization, which has long been known as the dominant decay process.[71,72] However, a stable chelate **1o**–Mg^{2+} (**1o′**) was formed in the presence of Mg^{2+}. The isomerization of C=N bond was inhibited, which increased the rigidity of the molecule, resulting in the chelation enhanced fluorescence (CHEF) effect.[73]

The fluorescence switching property of **1o′** was also investigated. As shown in Fig. 3B, the emission intensity of **1o′** gradually decreased with the irradiation of 297 nm light, due to the formation of closed-ring isomer **1c**–Mg^{2+} (**1c′**).[74] When the PSS was reached, the fluorescence of **1o′** was quenched by 37%, accompanied by the fluorescent color changed from green to dark green. Reversely, the fluorescence spectrum of **1o′** could be recovered upon irradiation with visible light (λ > 500 nm). In another way, the fluorescence spectral responses of the closed-ring isomer **1c** to Mg^{2+} were also studied (Fig. S7†). With the addition of Mg^{2+}, the emission intensity of **1c** was obviously enhanced, and the emission peak shifted from 442 nm to 552 nm. When the amount of Mg^{2+} reached 3.0 equivalents, the fluorescence spectrum was consistent with that from **1o′** with 297 nm light. Meanwhile, the fluorescent color changed from dark to dark green. Reversely, upon the addition of EDTA (10.0 equivalents of **1o**), the fluorescence spectrum of **1c′** recovered immediately to that of **1c**, showing that the complexation–decomplexation reaction between **1c** and Mg^{2+} was also reversible.

Additionally, to evaluate the effects of pH on the sensor, the fluorescence spectral changes of **1o**–Mg^{2+} over different pH values were also studied (Fig. S8†), the pH was adjusted by dropping an appropriate amount of the aqueous solution of HCl and NaOH into acetonitrile, and was measured with Ferromagnetic PHS-3C pH meter. The results showed the optimal pH range for the fluorescence emission of **1o**–Mg^{2+} is 7–9. At the same time, the experiments of fluorescence response of **1o** to $Mg(NO_3)_2$, $MgCl_2$, and $Mg(ClO_4)_2$ were also performed. As shown in Fig. S9,† the emission intensity of **1o** + $Mg(NO_3)_2$ was much higher than that of **1o** + $MgCl_2$ and **1o** + $Mg(ClO_4)_2$. The results indicated the counter anions have certain influence on the sensing of Mg^{2+}.

Complexation mechanism of 1o with Mg^{2+}

Job's plot analysis was performed to prove the complexation of **1o**–Mg^{2+} according to the previous report.[75] The result showed that the emission intensity approached the maximum when the molar fraction of $[Mg^{2+}]/([\mathbf{1o}] + [Mg^{2+}])$ was about 0.5, suggesting a 1 : 1 binding stoichiometry between **1o** and Mg^{2+} in acetonitrile (Fig. 4). Meanwhile, the binding constant (K_a) of **1o** and Mg^{2+} was determined to be 1.14×10^2 L mol^{-1} with the slope and intercept of the linearity ($R = 0.998$) (Fig. S10†). According to the reported method,[76] the limit of detection of **1o** toward Mg^{2+} was calculated to be 3.58×10^{-7} mol L^{-1} (Fig. S11†). Therefore, **1o** could serve as a highly sensitive fluorescent sensor for the detection of Mg^{2+} in acetonitrile.

Furthermore, ^{1}H NMR titration experiments were carried out in acetonitrile-d_3 to further prove the coordination of **1o** and Mg^{2+}. As shown in Fig. 5, with the addition of Mg^{2+}, the Hb signal displayed a downfield shift of 0.01 ppm from 6.84 ppm to 6.85 ppm, and the Ha resonance signal at 7.32 ppm disappeared completely, indicating the coordinated bond of O–Mg^{2+} was formed. At the same time, the Hc on the pyrimidine displayed a shift of 0.02 ppm from 8.40 ppm to 8.38 ppm, showing the formation of the coordinate bond of N–Mg^{2+}. These results indicated that the O of the hydroxyl group, the N of pyrimidine are the most likely binding sites. Moreover, the HRMS analysis was also carried out to confirm the interaction between **1o** and Mg^{2+}. The testing sample was prepared by adding Mg^{2+} to **1o** in acetonitrile, and the result indicated that a signal located at m/z = 663.0922 was consistent well with the ensemble $[\mathbf{1o} + Mg^{2+} + NO_3^-]^+$ (m/z calcd: 663.0987) (Fig. S12†). In addition, the IR spectral experiments of **1o** and **1o**–Mg^{2+} have been also performed at room temperature. As shown in Fig. S13,† the peak at 1608 cm^{-1} corresponds to C=N stretching. Upon the complexation of **1o** and Mg^{2+}, the peak at 1608 cm^{-1} shifted to 1635 cm^{-1} due to the rigidification of the imine bond. Besides, the peak at 3440 cm^{-1} assigned to the stretching vibration of –OH shifted to 3408 cm^{-1}. The strong absorption peak at 1383 cm^{-1} was attributed to the added NO_3^-. These results further proved that **1o** and Mg^{2+} formed the 1 : 1 complex.

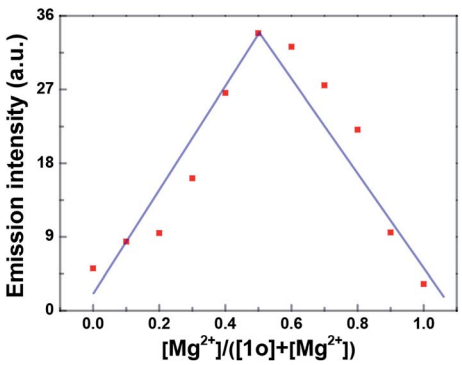

Fig. 4 Job's plot showing the 1 : 1 complex of **1o** and Mg^{2+} in acetonitrile (2.0×10^{-5} mol L^{-1}).

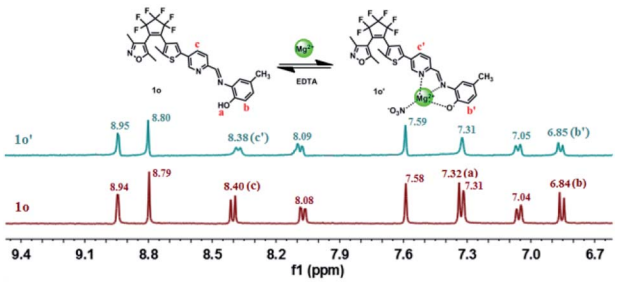

Fig. 5 Changes in ^{1}H NMR of **1o** and **1o**′ in acetonitrile-d_3 (Inset shows the proposed binding mode of **1o**′ complex).

Based on these results, the proposed binding mode was shown in Scheme 2.

Application in practical sample and logic circuit

To study the practical application ability of **1o** in Mg^{2+} detection, the competitive experiments for the fluorescence response of **1o** in the presence of Mg^{2+} and other metal ions were carried out in acetonitrile. As shown in Fig. S14,† the fluorescence response of **1o** to Mg^{2+} was not affected by other competing metal ions, expect for Cu^{2+}, Co^{2+}, Ni^{2+}. The results indicated that **1o** has reasonable anti-interference ability on sensing Mg^{2+} in acetonitrile. Meantime, the application of **1o** to real samples was also researched. The Mg^{2+} content in actual water samples from the Gan-Jiang River in Nanchang, Jiangxi province was measured. Table 1 showed the results determined with **1o** after the addition of a moderate amount of Mg^{2+}. The recoveries ranged from 94.3% to 103%. The results indicated that **1o** could be used to detect Mg^{2+} in real samples with high accuracy. Furthermore, on the basis of the photoswitching characteristics of **1o** modulated by either UV/vis lights or chemical reagents stimuli in acetonitrile, a logic circuit was constructed with four input signals including In1: 297 nm light, In2: >500 nm light, In3: Mg^{2+}, In4: EDTA and one output signal (Opt: emission intensity at 552 nm) (Fig. S15, Table S1†).[77,78] These results show that sensor **1o** has certain practical value in real sample detection and logic circuit.

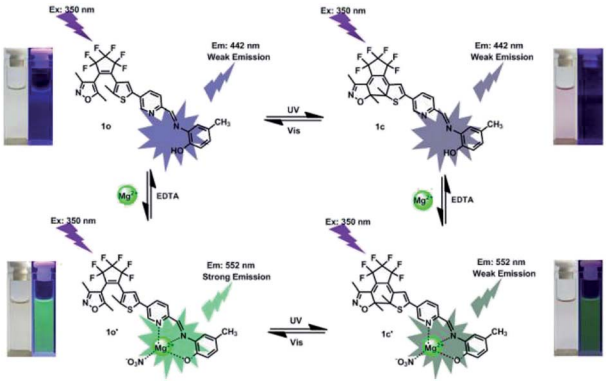

Scheme 2 Dual-controlled fluorescent-switching behavior of **1o** induced by Mg^{2+}/EDTA and UV/vis light.

Table 1 Application in actual water sample detection for Mg^{2+}

Sample no.	Mg^{2+} added (μM)	Mg^{2+} determined (μM)	Recovery (%)
1	4	4.11	103
2	8	7.63	95.4
3	12	11.32	94.3
4	16	16.39	102

Conclusions

In summary, a highly selective fluorescent sensor toward Mg^{2+} based on diarylethene and 4-methylphenol unit was successfully developed. This sensor exhibited outstanding photochromic and fluorescent switching properties in acetonitrile solution. The application results indicated that the sensor could be used to detect Mg^{2+} in real samples. Furthermore, a logic circuit was designed with the fluorescence intensity at 552 nm as output signal, the UV/vis lights and Mg^{2+}/EDTA as input signals. All of the results will be helpful for the design and synthesis of new sensors for the recognition of Mg^{2+} with high selectivity in the future.

Conflicts of interest

There are no conflicts of interest to declare.

Acknowledgements

The authors are grateful for the financial support from the National Natural Science Foundation of China (41867053), the "5511" science and technology innovation talent project of Jiangxi (2016BCB18015), the key project of Natural Science Foundation of Jiangxi Province (20171ACB20025), the Project of the Science Funds of the Education Office of Jiangxi (GJJ160773), the Young Talents Project of Jiangxi Science and Technology Normal University (2015QNBJRC004), the Project of Jiangxi Science and Technology Normal University Advantage Sci-Tech Innovative Team (2015CXTD002).

Notes and references

1 M. J. Cromie, Y. Shi and T. Latifi, *Cell*, 2006, **125**, 71–84.
2 G. Farruggia, S. Iotti and L. Prodi, *J. Am. Chem. Soc.*, 2006, **128**, 344–350.
3 L. Jin, Z. Guo and Z. Sun, *Sens. Actuators, B*, 2012, **161**, 714–720.
4 D. Ray, A. Nag and A. Jana, *Inorg. Chim. Acta*, 2010, **363**, 2824–2832.
5 B. O'Rourke, P. H. Backx and E. Marban, *Science*, 1992, **257**, 245–248.
6 C. Schmitz, A. L. Perraud and C. O. Johnson, *Cell*, 2003, **114**, 191–200.
7 Y. Zhao, A. M. Ren and L. Y. Zou, *Theor. Chem. Acc.*, 2011, **130**, 61.
8 S. Ishijima, A. Uchibori and H. Takagi, *Arch. Biochem. Biophys.*, 2003, **412**, 126–132.
9 H. C. Politi and R. R. Preston, *NeuroReport*, 2003, **14**, 659–668.
10 H. Rubin, *Arch. Biochem. Biophys.*, 2007, **458**, 16–23.
11 F. I. Wolf, A. Torsello and S. Fasanella, *Mol. Aspects Med.*, 2003, **24**, 11–26.
12 K. Seki, K. Aizawa and T. Sugaoi, *Chem. Lett.*, 2008, **37**, 872–873.
13 B. O'Rourke, P. H. Backx and E. Marban, *Science*, 1992, **257**, 245–248.
14 R. Bogoroch and L. F. Belanger, *Anat. Rec.*, 1975, **183**, 437–447.
15 H. O. Trowbridge and J. L. Seltzer, *J. Periodontal Res.*, 1967, **2**, 147–153.
16 L. Wang, W. Qin and X. Tang, *J. Phys. Chem. A*, 2011, **115**, 1609–1616.
17 N. E. L. Saris, E. Mervaala and H. Karppanen, *Clin. Chim. Acta*, 2000, **294**, 1–26.
18 J. A. M. Maier, *Mol. Aspects Med.*, 2003, **24**, 137–146.
19 M. Barbagallo and L. J. Dominguez, *Arch. Biochem. Biophys.*, 2007, **458**, 40–47.
20 T. Hashimoto, K. Nishi and J. Nagasao, *Brain Res.*, 2008, **1197**, 143–151.
21 R. Swaminathan, *Clin. Biochem. Rev.*, 2003, **24**, 47.
22 W. Jahnen-Dechent and M. Ketteler, *Clin. Kidney J.*, 2012, **5**, 3–14.
23 R. M. Touyz, *Front. Biosci.*, 2004, **9**, 1278–1293.
24 Y. Rayssiguier, E. Gueux and W. Nowacki, *Magnesium Res.*, 2006, **19**, 237–243.
25 M. Barbagallo, L. J. Dominguez and A. Galioto, *Mol. Aspects Med.*, 2003, **24**, 39–52.
26 J. Zhu, Y. Qin and Y. Zhang, *Anal. Chem.*, 2009, **82**, 436–440.
27 H. Hifumi, A. Tanimoto and D. Citterio, *Analyst*, 2007, **132**, 1153–1160.
28 M. Ishida, Y. Naruta and F. Tani, *Angew. Chem., Int. Ed.*, 2010, **49**, 91–94.
29 S. Patra and P. Paul, *Dalton Trans.*, 2009, **40**, 8683–8695.
30 K. B. Kim, H. Kim and E. J. Song, *Dalton Trans.*, 2013, **42**, 16569–16577.
31 S. Goswami, A. Manna and S. Paul, *Dalton Trans.*, 2013, **42**, 8078–8085.
32 V. K. Gupta, N. Mergu and L. K. Kumawat, *Sens. Actuators, B*, 2015, **207**, 216–223.
33 G. Farruggia, S. Iotti and L. Prodi, *J. Am. Chem. Soc.*, 2007, **129**, 1470.
34 H. Hama, T. Morozumi and H. Nakamura, *Tetrahedron Lett.*, 2007, **48**, 1859–1861.
35 K. C. Song, M. G. Choi and D. H. Ryu, *Tetrahedron Lett.*, 2007, **48**, 5397–5400.
36 H. M. Kim, P. R. Yang and M. S. Seo, *J. Org. Chem.*, 2007, **72**, 2088–2096.
37 Y. Liu, Z. Y. Duan and H. Y. Zhang, *J. Org. Chem.*, 2005, **70**, 1450–1455.
38 B. J. Sanghavi, W. Varhue and J. L. Chávez, *Anal. Chem.*, 2014, **86**, 4120–4125.

39 B. J. Sanghavi, S. Sitaula and M. H. Griep, *Anal. Chem.*, 2013, **85**, 8158–8165.
40 B. J. Sanghavi, S. M. Mobin and P. Mathur, *Biosens. Bioelectron.*, 2013, **39**, 124–132.
41 B. J. Sanghavi and A. K. Srivastava, *Electrochim. Acta*, 2010, **55**, 8638–8648.
42 B. J. Sanghavi and A. K. Srivastava, *Electrochim. Acta*, 2011, **56**, 4188–4196.
43 P. S. Hariharan and S. P. Anthony, *RSC Adv.*, 2014, **4**, 41565–41571.
44 H. Sharma, N. Kaur and A. Singh, *J. Mater. Chem. C*, 2016, **4**, 5154–5194.
45 V. K. Gupta, N. Mergu and L. K. Kumawat, *Sens. Actuators, B*, 2016, **223**, 101–113.
46 M. Liu, X. Yu and M. Li, *RSC Adv.*, 2018, **8**, 12573–12587.
47 G. T. Selvan, V. Chitra and V. M. V. Enoch Israel, *New J. Chem.*, 2018, **42**, 902–909.
48 J. H. Hu, J. B. Li and Y. Sun, *RSC Adv.*, 2017, **7**, 29697–29701.
49 Y. Ma, H. Liu and S. Liu, *Analyst*, 2012, **137**, 2313–2317.
50 G. Men, C. Chen and S. Zhang, *Dalton Trans.*, 2015, **44**, 2755–2762.
51 Q. Lin, J. J. Gruskos and D. Buccella, *Org. Biomol. Chem.*, 2016, **14**, 11381–11388.
52 X. Zhu, C. He and D. Dong, *Dalton Trans.*, 2010, **39**, 10051–10055.
53 G. Zhang, J. J. Gruskos and M. S. Afzal, *Chem. Sci.*, 2015, **6**, 6841–6846.
54 G. Wang, J. Qin and L. Fan, *J. Photochem. Photobiol., A*, 2016, **314**, 29–34.
55 M. Irie, T. Fukaminato, T. Sasaki, N. Tamai and T. Kawai, *Nature*, 2002, **420**, 759.
56 H. Tian and S. Yang, *Chem. Soc. Rev.*, 2004, **33**, 85–97.
57 K. Matsuda and M. Irie, *J. Photochem. Photobiol., C*, 2004, **5**, 169–182.
58 S. Z. Pu, H. Ding and G. Liu, *J. Phys. Chem. C*, 2014, **118**, 7010–7017.
59 Q. Zou, X. Li and J. Zhang, *Chem. Commun.*, 2012, **48**, 2095–2097.
60 H. Liu and Y. Chen, *Eur. J. Org. Chem.*, 2009, **30**, 5261–5265.
61 Q. Zou, J. Jin and B. Xu, *Tetrahedron*, 2011, **67**, 915–921.
62 Z. Zhou, H. Yang and M. Shi, *ChemPhysChem*, 2007, **8**, 1289–1292.
63 Z. Zhou, S. Xiao and J. Xu, *Org. Lett.*, 2006, **8**, 3911–3914.
64 Z. Li, C. Zhang and Y. Ren, *Org. Lett.*, 2011, **13**, 6022–6025.
65 S. Z. Pu, D. Jiang and W. Liu, *J. Mater. Chem.*, 2012, **22**, 3517–3526.
66 S. Q. Cui, Z. Tian and S. Z. Pu, *RSC Adv.*, 2016, **6**, 19957–19963.
67 S. Z. Pu, Z. P. Tong, G. Liu and R. J. Wang, *J. Mater. Chem. C*, 2013, **1**, 4726–4739.
68 M. Irie, *Chem. Rev.*, 2000, **100**, 1685–1716.
69 Z. X. Li, L. Y. Liao and W. Sun, *J. Phys. Chem. C*, 2008, **112**, 5190–5196.
70 S. Z. Pu, J. Xu and L. Shen, *Tetrahedron Lett.*, 2005, **46**, 871–875.
71 Z. Wang, S. Q. Cui, S. Y. Qiu and S. Z. Pu, *Spectrochim. Acta, Part A*, 2018, **205**, 21–28.
72 W. K. Dong, X. L. Li, L. Wang, Y. Zhang and Y. J. Ding, *Sens. Actuators, B*, 2016, **229**, 370–378.
73 E. T. Feng, Y. Y. Tu, C. B. Fan, G. Liu and S. Z. Pu, *RSC Adv.*, 2017, **7**, 50188–50194.
74 Z. Wang, S. Q. Cui, S. Y. Qiu and S. Z. Pu, *RSC Adv.*, 2018, **8**, 29295–29300.
75 J. S. Wu, W. M. Liu and X. Q. Zhuang, *Org. Lett.*, 2007, **9**, 33–36.
76 H. Wang, B. Wang and Z. Shi, *Biosens. Bioelectron.*, 2015, **65**, 91–96.
77 Z. Wang, S. Q. Cui, S. Y. Qiu and S. Z. Pu, *J. Photochem. Photobiol., A*, 2018, **367**, 212–218.
78 Z. Wang, S. Q. Cui, S. Y. Qiu and S. Z. Pu, *Tetrahedron*, 2018, **74**, 7431–7437.